



UvA-DARE (Digital Academic Repository)

Measurement of the average lifetime of b hadrons

Adriani, O.; Aguilar-Benitez, M.; Ahlen, S.P.; Alcaraz, J.; Aloisio, A.; Alverson, G.; Alvigi, M.G.; Ambrosi, G.; Linde, F.L.

Published in:
Physics Letters B

DOI:
[10.1016/0370-2693\(93\)91027-K](https://doi.org/10.1016/0370-2693(93)91027-K)

[Link to publication](#)

Citation for published version (APA):

Adriani, O., Aguilar-Benitez, M., Ahlen, S. P., Alcaraz, J., Aloisio, A., Alverson, G., ... Linde, F. L. (1993). Measurement of the average lifetime of b hadrons. *Physics Letters B*, 317, 474-484. DOI: 10.1016/0370-2693(93)91027-K

General rights

It is not permitted to download or to forward/distribute the text or part of it without the consent of the author(s) and/or copyright holder(s), other than for strictly personal, individual use, unless the work is under an open content license (like Creative Commons).

Disclaimer/Complaints regulations

If you believe that digital publication of certain material infringes any of your rights or (privacy) interests, please let the Library know, stating your reasons. In case of a legitimate complaint, the Library will make the material inaccessible and/or remove it from the website. Please Ask the Library: <http://uba.uva.nl/en/contact>, or a letter to: Library of the University of Amsterdam, Secretariat, Singel 425, 1012 WP Amsterdam, The Netherlands. You will be contacted as soon as possible.

Measurement of the average lifetime of b hadrons

L3 Collaboration

O. Adriani^o, M. Aguilar-Benitez^x, S. Ahlen^l, J. Alcaraz^p, A. Aloisio^{aa}, G. Alverson^j, M.G. Alviggi^{aa}, G. Ambrosi^{af}, Q. An^q, H. Anderhub^{at}, A.L. Andersonⁿ, V.P. Andreev^{aj}, T. Angelescu^k, L. Antonov^{an}, D. Antreasyan^g, P. Arce^x, A. Arefiev^z, A. Atamanchuk^{aj}, T. Azemoon^c, T. Aziz^h, P.V.K.S. Baba^q, P. Bagnaia^{ai}, J.A. Bakken^{ah}, R.C. Ball^c, S. Banerjee^h, J. Bao^e, R. Barillère^p, L. Barone^{ai}, A. Baschirotto^y, R. Battiston^{af}, A. Bay^r, F. Becattini^o, J. Bechtluft^a, R. Becker^a, U. Becker^{n,at}, F. Behner^{at}, J. Behrens^{at}, Gy.L. Bencze^l, J. Berdugo^x, P. Bergesⁿ, B. Bertucci^{af}, B.L. Betev^{an,at}, M. Biasini^{af}, A. Biland^{at}, G.M. Bilei^{af}, R. Bizzarri^{ai}, J.J. Blaising^d, G.J. Bobbink^{p,b}, R. Bock^a, A. Böhm^a, B. Borgia^{ai}, M. Bosetti^y, D. Bourilkov^{ac}, M. Bourquin^r, D. Boutigny^p, B. Bouwens^b, E. Brambilla^{aa}, J.G. Branson^{ak}, I.C. Brock^{ag}, M. Brooks^v, A. Bujak^{aq}, J.D. Burgerⁿ, W.J. Burger^r, J. Busenitz^{ap}, A. Buytenhuijs^{ac}, X.D. Cai^q, M. Capellⁿ, M. Caria^{af}, G. Carlino^{aa}, A.M. Cartacci^o, R. Castello^y, M. Cerrada^x, F. Cesaroni^{ai}, Y.H. Changⁿ, U.K. Chaturvedi^q, M. Chemarin^w, A. Chen^{av}, C. Chen^f, G. Chen^f, G.M. Chen^f, H.F. Chen^s, H.S. Chen^f, M. Chenⁿ, W.Y. Chen^{av}, G. Chiefari^{aa}, C.Y. Chien^e, M.T. Choi^{ao}, S. Chungⁿ, C. Civinini^o, I. Clareⁿ, R. Clareⁿ, T.E. Coan^v, H.O. Cohn^{ad}, G. Coignet^d, N. Colino^p, A. Contin^g, S. Costantini^{ai}, F. Cotorobai^k, X.T. Cui^q, X.Y. Cui^q, T.S. Daiⁿ, R. D'Alessandro^o, R. de Asmundis^{aa}, A. Degré^d, K. Deiters^{ar}, E. Dénes^l, P. Denes^{ah}, F. DeNotaristefani^{ai}, M. Dhina^{at}, D. DiBitonto^{ap}, M. Diemoz^{ai}, H.R. Dimitrov^{an}, C. Dionisi^{ai}, M. Dittmar^{at}, L. Djambazov^{at}, M.T. Dova^q, E. Drago^{aa}, D. Duchesneau^r, P. Duinker^b, I. Duran^{af}, S. Easo^{af}, H. El Mamouni^w, A. Engler^{ag}, F.J. Epplingⁿ, F.C. Erné^b, P. Extermann^r, R. Fabbretti^{ar}, M. Fabre^{ar}, S. Falciano^{ai}, S.J. Fan^{am}, O. Fackler^u, J. Fay^w, M. Felcini^p, T. Ferguson^{ag}, D. Fernandez^x, G. Fernandez^x, F. Ferroni^{ai}, H. Fesefeldt^a, E. Fiandrini^{af}, J.H. Field^r, F. Filthaut^{ac}, P.H. Fisher^e, G. Forconi^r, L. Fredj^r, K. Freudenreich^{at}, W. Friebel^{as}, M. Fukushimaⁿ, M. Gailloud^t, Yu. Galaktionov^{z,n}, E. Gallo^o, S.N. Ganguli^{p,h}, P. Garcia-Abia^x, D. Gele^w, S. Gentile^{ai}, N. Gheordanescu^k, S. Giagu^{ai}, S. Goldfarb^t, Z.F. Gong^s, E. Gonzalez^x, A. Gougas^e, D. Goujon^r, G. Gratta^{ae}, M. Gruenewald^p, C. Gu^q, M. Guanziroli^q, J.K. Guo^{am}, V.K. Gupta^{ah}, A. Gurtu^h, H.R. Gustafson^c, L.J. Gutay^{aq}, K. Hangarter^a, B. Hartmann^a, A. Hasan^q, D. Hauschildt^b, C.F. He^{am}, J.T. He^f, T. Hebbeker^p, M. Hebert^{ak}, A. Hervé^p, K. Hilgers^a, H. Hofer^{at}, H. Hoorani^r, G. Hu^q, G.Q. Hu^{am}, B. Ille^w, M.M. Ilyas^q, V. Innocente^p, H. Janssen^p, S. Jezequel^d, B.N. Jin^f, L.W. Jones^c, I. Josa-Mutuberría^p, A. Kasser^t, R.A. Khan^q, Yu. Kamyshkov^{ad}, P. Kapinos^{aj,as}, J.S. Kapustinsky^v, Y. Karyotakis^p, M. Kaur^q, S. Khokhar^q, M.N. Kienzle-Focacci^r, J.K. Kim^{ao}, S.C. Kim^{ao}, Y.G. Kim^{ao}, W.W. Kinnison^v, A. Kirkby^{ae}, D. Kirkby^{ae}, S. Kirsch^{as}, W. Kittel^{ac}, A. Klimentov^{n,z}, R. Klöckner^a, A.C. König^{ac}, E. Koffeman^b, O. Kornadt^a, V. Koutsenko^{n,z}, A. Koulbardiš^{aj}, R.W. Kraemer^{ag}, T. Kramerⁿ, V.R. Krastev^{an,af}, W. Krenz^a, A. Krivshich^{aj}, H. Kuijten^{ac}, K.S. Kumar^m, A. Kunin^{n,z}, G. Landi^o, D. Lanske^a, S. Lanzano^{aa}, A. Lebedevⁿ, P. Lebrun^w, P. Lecomte^{at}, P. Lecoq^p, P. Le Coultre^{at}, D.M. Lee^v, J.S. Lee^{ao}, K.Y. Lee^{ao}, I. Leedom^j, C. Leggett^c, J.M. Le Goff^p, R. Leiste^{as}, M. Lenti^o, E. Leonardi^{ai}, C. Li^{s,q}, H.T. Li^f, P.J. Li^{am}, J.Y. Liao^{am}, W.T. Lin^{av}, Z.Y. Lin^s, F.L. Linde^b, B. Lindemann^a, L. Lista^{aa}, Y. Liu^q, W. Lohmann^{as}, E. Longo^{ai}, Y.S. Lu^f, J.M. Lubbers^p, K. Lübelsmeyer^a, C. Luci^{ai}, D. Luckey^{g,n}, L. Ludovici^{ai},

L. Luminari^{ai}, W. Luster^{as}, J.M. Ma^f, W.G. Ma^s, M. MacDermott^{at}, R. Malik^q,
 A. Malinin^z, C. Mañá^x, M. Maolinbay^{at}, P. Marchesini^{at}, F. Marion^d, A. Marin^l, J.P. Martin^w,
 L. Martinez-Laso^x, F. Marzano^{ai}, G.G.G. Massaro^b, K. Mazumdar^r, P. McBride^m,
 T. McMahon^{aq}, D. McNally^{at}, M. Merk^{ag}, L. Merola^{aa}, M. Meschini^o, W.J. Metzger^{ac}, Y. Mi^t,
 A. Mihul^k, G.B. Mills^v, Y. Mir^q, G. Mirabelli^{ai}, J. Mnich^a, M. Möller^a, B. Monteleoni^o,
 R. Morand^d, S. Morganti^{ai}, N.E. Moulai^q, R. Mount^{ae}, S. Müller^a, A. Nadtochy^{aj}, E. Nagy^l,
 M. Napolitano^{aa}, F. Nessi-Tedaldi^{at}, H. Newman^{ae}, C. Neyer^{at}, M.A. Niaz^q, A. Nippe^a,
 H. Nowak^{as}, G. Organtini^{ai}, D. Pandoulas^a, S. Paoletti^{ai}, P. Paolucci^{aa}, G. Pascale^{ai},
 G. Passaleva^{o,af}, S. Patricelli^{aa}, T. Paul^e, M. Pauluzzi^{af}, C. Paus^a, F. Pauss^{at}, Y.J. Pei^a,
 S. Pensotti^y, D. Perret-Gallix^d, J. Perrier^r, A. Pevsner^e, D. Piccolo^{aa}, M. Pieri^p, P.A. Piroué^{ah},
 F. Plasil^{ad}, V. Plyaskin^z, M. Pohl^{at}, V. Pojidaev^{z,o}, H. Postemaⁿ, Z.D. Qi^{am}, J.M. Qian^c,
 K.N. Qureshi^q, R. Raghavan^h, G. Rahal-Callot^{at}, P.G. Rancoita^y, M. Rattaggi^y, G. Raven^b,
 P. Razis^{ab}, K. Read^{ad}, D. Ren^{at}, Z. Ren^q, M. Rescigno^{ai}, S. Reucroft^j, A. Ricker^a, S. Riemann^{as},
 B.C. Riemers^{aq}, K. Riles^c, O. Rind^c, H.A. Rizvi^q, S. Ro^{ao}, F.J. Rodriguez^x, B.P. Roe^c,
 M. Röhner^a, L. Romero^x, S. Rosier-Lees^d, R. Rosmalen^{ac}, Ph. Rosselet^t, W. van Rossum^b,
 S. Roth^a, A. Rubbiaⁿ, J.A. Rubio^p, H. Rykaczewski^{at}, M. Sachwitz^{as}, J. Salicio^p, J.M. Salicio^x,
 G.S. Sanders^v, A. Santocchia^{af}, M.S. Sarakinosⁿ, G. Sartorelli^{g,q}, M. Sassowsky^a, G. Sauvage^d,
 V. Schegelsky^{aj}, D. Schmitz^a, P. Schmitz^a, M. Schneegans^d, H. Schopper^{au}, D.J. Schotanus^{ac},
 S. Shotkinⁿ, H.J. Schreiber^{as}, J. Shukla^{ag}, R. Schulte^a, S. Schulte^a, K. Schultze^a, J. Schwenke^a,
 G. Schwering^a, C. Sciacca^{aa}, I. Scott^m, R. Sehgal^q, P.G. Seiler^{ar}, J.C. Sens^{p,b}, L. Servoli^{af},
 I. Sheer^{ak}, D.Z. Shen^{am}, S. Shevchenko^{ae}, X.R. Shi^{ae}, E. Shumilov^z, V. Shoutko^z, D. Son^{ao},
 A. Sopczak^p, V. Soulimov^{aa}, C. Spartiotis^e, T. Spickermann^a, P. Spillantini^o, R. Starosta^a,
 M. Steuer^{g,n}, D.P. Stickland^{ah}, F. Sticozziⁿ, H. Stone^{ah}, K. Strauch^m, B.C. Stringfellow^{aq},
 K. Sudhakar^h, G. Sultanov^q, L.Z. Sun^{s,q}, G.F. Susinno^r, H. Suter^{at}, J.D. Swain^q, A.A. Syed^{ac},
 X.W. Tang^f, L. Taylor^j, G. Terzi^y, Samuel C.C. Tingⁿ, S.M. Tingⁿ, M. Tonutti^a, S.C. Tonwar^h,
 J. Tóth^l, A. Tsaregorodtsev^{aj}, G. Tsipolitis^{ag}, C. Tully^{ah}, K.L. Tung^f, J. Ulbricht^{at}, L. Urbán^l,
 U. Uwer^a, E. Valente^{ai}, R.T. Van de Walle^{ac}, I. Vetlitsky^z, G. Viertel^{at}, P. Vikas^q, U. Vikas^q,
 M. Vivargent^d, H. Vogel^{ag}, H. Vogt^{as}, I. Vorobiev^{m,z}, A.A. Vorobyov^{aj}, L. Vuilleumier^t,
 M. Wadhwa^d, W. Wallraff^a, C. Wangⁿ, C.R. Wang^s, X.L. Wang^s, Y.F. Wangⁿ, Z.M. Wang^{q,s},
 C. Warner^a, A. Weber^a, J. Weber^{at}, R. Weill^t, T.J. Wenaus^u, J. Wenninger^r, M. Whiteⁿ,
 C. Willmott^x, F. Wittgenstein^p, D. Wright^{ah}, S.X. Wu^q, S. Wynhoff^a, B. Wyslouchⁿ,
 Y.Y. Xie^{am}, J.G. Xu^f, Z.Z. Xu^s, Z.L. Xue^{am}, D.S. Yan^{am}, B.Z. Yang^s, C.G. Yang^f, G. Yang^q,
 C.H. Ye^q, J.B. Ye^s, Q. Ye^q, S.C. Yeh^{av}, Z.W. Yin^{am}, J.M. You^q, N. Yunus^q, M. Yzerman^b,
 C. Zaccardelli^{ae}, N. Zaitsev^{aa}, P. Zemp^{at}, M. Zeng^q, Y. Zeng^a, D.H. Zhang^b, Z.P. Zhang^{s,q},
 B. Zhou^l, G.J. Zhou^f, J.F. Zhou^a, R.Y. Zhu^{ae}, A. Zichichi^{g,p,q} and B.C.C. van der Zwaan^b

^a I. Physikalisches Institut, RWTH, W-5100 Aachen, FRG¹

and III. Physikalisches Institut, RWTH, W-5100 Aachen, FRG¹

^b National Institute for High Energy Physics, NIKHEF, NL-1009 DB Amsterdam, The Netherlands

^c University of Michigan, Ann Arbor, MI 48109, USA

^d Laboratoire d'Annecy-le-Vieux de Physique des Particules, LAPP, IN2P3-CNRS,
 BP 110, F-74941 Annecy-le-Vieux Cedex, France

^e Johns Hopkins University, Baltimore, MD 21218, USA

^f Institute of High Energy Physics, IHEP, 100039 Beijing, China

^g INFN – Sezione di Bologna, I-40126 Bologna, Italy

^h Tata Institute of Fundamental Research, Bombay 400 005, India

ⁱ Boston University, Boston, MA 02215, USA

^j Northeastern University, Boston, MA 02115, USA

^k Institute of Atomic Physics and University of Bucharest, R-76900 Bucharest, Romania

^l Central Research Institute for Physics of the Hungarian Academy of Sciences, H-1525 Budapest 114, Hungary²

- ^m *Harvard University, Cambridge, MA 02139, USA*
ⁿ *Massachusetts Institute of Technology, Cambridge, MA 02139, USA*
^o *INFN – Sezione di Firenze and University of Florence, I-50125 Florence, Italy*
^p *European Laboratory for Particle Physics, CERN, CH-1211 Geneva 23, Switzerland*
^q *World Laboratory, FBLJA Project, CH-1211 Geneva 23, Switzerland*
^r *University of Geneva, CH-1211 Geneva 4, Switzerland*
^s *Chinese University of Science and Technology, USTC, Hefei, Anhui 230 029, China*
^t *University of Lausanne, CH-1015 Lausanne, Switzerland*
^u *Lawrence Livermore National Laboratory, Livermore, CA 94550, USA*
^v *Los Alamos National Laboratory, Los Alamos, NM 87544, USA*
^w *Institut de Physique Nucléaire de Lyon, IN2P3-CNRS, Université Claude Bernard, F-69622 Villeurbanne Cedex, France*
^x *Centro de Investigaciones Energeticas, Medioambientales y Tecnológicas, CIEMAT, E-28040 Madrid, Spain*
^y *INFN – Sezione di Milano, I-20133 Milan, Italy*
^z *Institute of Theoretical and Experimental Physics, ITEP, Moscow, Russia*
^{aa} *INFN – Sezione di Napoli and University of Naples, I-80125 Naples, Italy*
^{ab} *Department of Natural Sciences, University of Cyprus, Nicosia, Cyprus*
^{ac} *University of Nymegen and NIKHEF, NL-6525 ED Nymegen, The Netherlands*
^{ad} *Oak Ridge National Laboratory, Oak Ridge, TN 37831, USA*
^{ae} *California Institute of Technology, Pasadena, CA 91125, USA*
^{af} *INFN-Sezione di Perugia and Università Degli Studi di Perugia, I-06100 Perugia, Italy*
^{ag} *Carnegie Mellon University, Pittsburgh, PA 15213, USA*
^{ah} *Princeton University, Princeton, NJ 08544, USA*
^{ai} *INFN-Sezione di Roma and University of Rome, “La Sapienza”, I-00185 Rome, Italy*
^{aj} *Nuclear Physics Institute, St Petersburg, Russia*
^{ak} *University of California, San Diego, CA 92093, USA*
^{al} *Departamento de Física de Partículas Elementales, Universidad de Santiago, E-15706 Santiago de Compostela, Spain*
^{am} *Shanghai Institute of Ceramics, SIC, Shanghai, China*
^{an} *Bulgarian Academy of Sciences, Institute of Mechatronics, BU-1113 Sofia, Bulgaria*
^{ao} *Center for High Energy Physics, Korea Advanced Institute of Sciences and Technology, 305-701 Taejeon, South Korea*
^{ap} *University of Alabama, Tuscaloosa, AL 35486, USA*
^{aq} *Purdue University, West Lafayette, IN 47907, USA*
^{ar} *Paul Scherrer Institut, PSI, CH-5232 Villigen, Switzerland*
^{as} *DESY-Institut für Hochenergiephysik, O-1615 Zeuthen, FRG*
^{at} *Eidgenössische Technische Hochschule, ETH Zürich, CH-8093 Zürich, Switzerland*
^{au} *University of Hamburg, W-2000 Hamburg, FRG*
^{av} *High Energy Physics Group, Taiwan, ROC*

Received 30 August 1993

Editor: K. Winter

The average lifetime of b hadrons has been measured using the L3 detector at LEP, running at $\sqrt{s} \approx M_Z$. A b-enriched sample was obtained from 432 538 hadronic Z events collected in 1990 and 1991 by tagging electrons and muons from semileptonic b hadron decays. From maximum likelihood fits to the electron and muon impact parameter distributions, the average b hadron lifetime was measured to be $\tau_b = (1535 \pm 35 \pm 28)$ fs, where the first error is statistical and the second includes both the experimental and the theoretical systematic uncertainties.

1. Introduction

The measurement of the lifetimes and semileptonic branching ratios of b hadrons enables the determination of the Cabibbo–Kobayashi–Maskawa matrix element $|V_{cb}|$. Measurements of the average b hadron lifetime τ_b have previously been made at PEP [1],

¹ Supported by the German Bundesministerium für Forschung und Technologie.

² Supported by the Hungarian OTKA fund under contract number 2970.

PETRA [2], and LEP [3,4].

In this analysis τ_b has been measured using a sample of 432 538 hadronic Z decays recorded during the 1990 and 1991 LEP runs with the L3 detector. A sample of events was selected which was enriched with b hadrons decaying semileptonically to either an electron or a muon. The average b hadron lifetime was then obtained from a likelihood fit to the projected impact parameter distribution of the lepton tracks. A general description of the impact parameter method may be found in ref. [5]; this analysis is described in more detail in ref. [6]. The measured b lifetime is an average of the lifetimes of the different types of b hadron produced in Z decays, weighted by their relative production rates and semileptonic branching ratios. Due to the higher statistics and the improvements in the analysis method, detector understanding, and the treatment of the tracking resolution, this measurement supersedes the previous L3 result [4].

2. The L3 detector

The L3 detector is described in detail in ref. [7]. The central tracking chamber is a Time Expansion Chamber (TEC) consisting of two coaxial cylindrical drift chambers with 12 inner and 24 outer sectors [8]. The Z-chamber surrounding the TEC consists of two coaxial proportional chambers with cathode strip readout. The electromagnetic calorimeter is composed of bismuth germanate (BGO) crystals. Hadronic energy depositions are measured by a uranium-proportional wire chamber sampling calorimeter surrounding the BGO. Scintillator timing counters are located between the electromagnetic and hadronic calorimeters. The muon spectrometer, located outside the hadron calorimeter, consists of three layers of drift chambers measuring the muon trajectory in both the bending and the non-bending planes. All subdetectors are installed inside a large magnet which provides a uniform field of 0.5 T.

The TEC has a projected impact parameter resolution of $109 \mu\text{m}$ for tracks in dilepton events, a transverse momentum resolution of $\sigma(1/p_T^{\text{TEC}}) = 0.022/\text{GeV}$, and an azimuthal angular resolution of 1 mrad at the face of the BGO. The BGO energy resolution for electrons of more than 1 GeV is better than 2% and the space angle resolution is approximately

3 mrad. At 45 GeV the muon chamber momentum resolution is 2.8%.

3. Inclusive lepton selection

Events were required to satisfy the online trigger and offline hadronic event selection criteria [9]. For the combined 1990 and 1991 data samples, 432 538 events passed the hadronic selection cuts with an efficiency of better than 99% and negligible contamination. Requiring in addition that the BGO calorimeter and muon chambers were fully operational resulted in samples of 412 460 and 407 534 hadronic events for the electron and muon analyses respectively.

Electron candidates were required to be in the BGO barrel ($|\cos\theta| < 0.69$) and to have a lateral BGO shower shape consistent with an electromagnetic energy deposit. The BGO cluster and TEC track had to match in azimuth to within 5 mrad (≈ 3 standard deviations) to ensure that the cluster was caused by a charged particle. The energy of a hadron shower in the BGO is, under the electron hypothesis, typically half the true hadron energy. The hadronic background was therefore strongly suppressed by requiring that the transverse BGO energy and the transverse momentum of the TEC track match to within 3 standard deviations. The energy deposited in the hadron calorimeter within a cone of half angle 7° around the BGO cluster was required to be less than 3 GeV. This cut further suppresses the hadronic background and rejects photons from π^0/η decays which are accompanied by a charged hadron. The background from photon conversions is relatively low due to the small amount of material preceding TEC ($\sim 1\%$ of a radiation length).

Muon candidate tracks in the muon spectrometer were required to have hits in at least two of the three $r\phi$ layers and at least one of the two z layers. The dominant background of punchthrough hadrons was suppressed by requiring the muon chamber track to point towards the primary vertex and to match in the $r\phi$ plane with a TEC track to within 75 mrad. The background from decays in flight ($\pi^\pm/K^\pm \rightarrow \mu^\pm$) is relatively low due to the small diameter of TEC. Contamination due to cosmic rays which coincide with a genuine hadronic event was reduced to a negligible

Table 1
Composition of the inclusive electron and muon samples.

Fraction, f_j , of the total sample	Electrons	Muons
f_b (prompt $b \rightarrow \ell$)	80.3%	79.9%
f_{bc} (cascade $b \rightarrow c, \tau, J, \bar{c} \rightarrow \ell$)	7.3%	6.8%
f_c (prompt $c \rightarrow \ell$)	3.2%	4.5%
f_{bkg} (background)	9.2%	8.8%

level by scintillator timing cuts and the vertex matching requirements.

The tracks of electron and muon candidates were required to have hits in both the inner and outer TEC sectors and to have azimuthal angles larger than 30 mrad and 15 mrad from the inner and outer TEC anode planes respectively to remove tracks in the low resolution drift gaps of TEC. The characteristically hard fragmentation and high mass of b quarks was exploited to enhance the b purity of the sample. Selected electrons and muons had to have an energy of more than 3 GeV. The momentum transverse to the nearest jet, p_T^{jet} , was required to be greater than 1.0 GeV and 1.4 GeV respectively for electrons and muons.

After applying these selection criteria 2998 electron and 4359 muon candidates remained. The compositions of the inclusive lepton samples were estimated using a sample of approximately 1.2×10^6 hadronic Z events which were generated using the JETSET 7.3 Monte Carlo [10] passed through the L3 detector simulation program^{#1} and then fully reconstructed. JETSET was tuned to reproduce the inclusive lepton spectra, measured by ARGUS and CLEO [13] at the $\Upsilon(4S)$ resonance and by DELCO and MARK III [14] at the $\psi(3770)$ resonance, by adjusting the rates of D^{**} and K^* mesons produced in b and c decays. This also partially corrected the inadequate Monte Carlo modelling of multibody final states in b and c decays. Table 1 summarises the compositions of the inclusive lepton samples. The prompt and cascade b decays, which constitute 87% of the sample, are both sensitive to τ_b .

^{#1} The L3 detector simulation program is based on the GEANT program [11]. Hadronic interactions in the detector were modelled using GHEISHA [12]. Events were corrected for the TEC, BGO and muon chamber inefficiencies obtained from the data.

4. Lifetime fitting method

Fig. 1 illustrates the definition of the impact parameter δ used in this analysis. It is defined to be the perpendicular distance of the lepton track from the centroid of the LEP beam intersection region, projected onto the plane normal to the beam where the beam spot size and the tracking errors are relatively small. In the highly relativistic limit, δ is approximately independent of the momentum of the b hadron and scales with the proper lifetime. The b hadron direction of flight was approximated, to an accuracy of better than 2.5° , by the thrust axis of the jet closest to the lepton. The sign of δ was taken to be positive if the angle between the jet axis vector and the vector joining the beam centroid and the projected b decay point was less than 90° , otherwise it was taken to be negative. For particles from the primary event vertex, δ is zero on average with a symmetric spread due to the experimental resolution and the beam spot size. For the decay products of b hadrons and other long-lived particles δ is on average positive.

The b hadron lifetime was obtained from an unbinned maximum likelihood fit to the measured impact parameter distribution with τ_b as the only free parameter. The likelihood for each track is a sum of the probability distributions for the four components of the sample weighted by their relative fractions (as given in table 1). The total likelihood function, $\mathcal{L}(\tau_b)$, is then

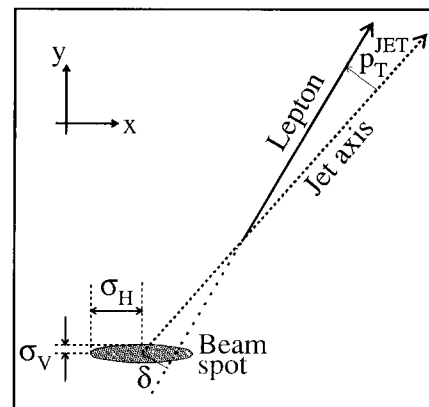


Fig. 1. Definition of the lepton impact parameter, δ .

$$\mathcal{L}(\tau_b) = \prod_{i \text{ lepton candidates}} \left[\left(f_b \mathcal{P}_b(\tau_b; \delta_i) + f_{bc} \mathcal{P}_{bc}(\tau_b; \delta_i) + f_c \mathcal{P}_c(\delta_i) \right) \otimes \mathcal{R}(\delta_i, \phi_i, p_{T,i}^{\text{TEC}}, \sigma_{\text{fit},i}) + f_{\text{bkg}} \mathcal{B}(\delta_i) \right]. \quad (1)$$

\mathcal{P}_b , \mathcal{P}_{bc} , and \mathcal{P}_c are the impact parameter distributions for the prompt, cascade and charm components. They include the effects of lifetime and the occasional mis-signing of δ , due to the approximation of the b hadron direction by the jet axis, but not the beam spot size nor the track measurement errors. \mathcal{P}_b , \mathcal{P}_{bc} , and \mathcal{P}_c are known collectively as the underlying distributions. \mathcal{R} is the track-by-track impact parameter resolution function which depends on the track azimuthal angle ϕ_i , the momentum $p_{T,i}^{\text{TEC}}$ transverse to the beam, and the impact parameter error from the track fit $\sigma_{\text{fit},i}$. \mathcal{B} is the impact parameter distribution for background tracks. The resolution function and the underlying and background distributions are described below. Separate fits were made to the impact parameter distributions of the inclusive electron and muon samples for all measured impact parameters in the range $|\delta| < 5$ mm.

The underlying distributions were obtained by applying the inclusive lepton selections to JETSET Monte Carlo event samples. To reduce uncertainties from limited Monte Carlo statistics, the hadronic event sample was supplemented by two additional samples, each of $10^5 Z \rightarrow b\bar{b}$ events. In one sample either one of the b hadrons was forced to decay semileptonically to an electron and in the other sample one b hadron was forced to decay to a muon. Each underlying distribution was parametrised separately for the $\delta < 0$ and $\delta > 0$ regions by a sum of exponential functions. A correction for the effect of final state bremsstrahlung on the electron impact parameter was estimated using a modified version of the KORALZ Monte Carlo program [15] and applied to the inclusive electron sample.

5. Impact parameter resolution

The impact parameter resolution includes contributions from the beam spot size, the TEC resolution,

and multiple Coulomb scattering in the beam pipe and TEC inner wall. Systematic errors in the impact parameter measurement were determined as a function of azimuthal angle using Bhabha and dimuon events. Applying the resulting corrections improved the average impact parameter resolution from $117 \mu\text{m}$ to $109 \mu\text{m}$. These corrections were applied to all inclusive lepton tracks. The multiple scattering contribution σ_{MS} was parametrised in terms of p_T^{TEC} by: $\sigma_{\text{MS}} = \kappa/p_T^{\text{TEC}}$, with $\kappa = 97 \mu\text{m GeV}$ and $76 \mu\text{m} \cdot \text{GeV}$ respectively for the 1990 and 1991 detector configurations.

The position of the beam centroid was measured using tracks from blocks of 100 consecutive hadronic events, with an accuracy of $30 \mu\text{m}$ in x and y , using a method which was insensitive to secondary decays. The beam positions were then smoothed assuming that the beam drifts were continuous with occasional discrete steps due to beam orbit corrections. The resulting accuracy in the beam position was estimated to be $10 \mu\text{m}$ in both x and y .

The one standard deviation horizontal and vertical beam spot dimensions, σ_H and σ_V , were measured using Bhabha and dimuon events. The beam spot size was obtained from a fit to the variance of the impact parameter distribution as a function of azimuthal angle, allowing for the contribution of the sector-dependent TEC resolution which was measured from the miss distance of pairs of tracks in dilepton events. The measured dimensions were $\sigma_H = (157 \pm 3) \mu\text{m}$ and $\sigma_V = (23 \pm 10) \mu\text{m}$.

The impact parameter resolution is somewhat degraded for tracks in multi-hadron events, compared to dilepton events, due to large angle multiple Coulomb scattering and the swapping or loss of hits due to neighbouring tracks. The resolution for the i th track was therefore parametrised by the sum of three Gaussians, with relative weights f_j and variances σ_{ij}^2 ($j = 1-3$), which describe in turn the well-measured, the poorly-measured, and the pathological tracks:

$$\mathcal{R}(\delta_i, \phi_i, p_{T,i}^{\text{TEC}}, \sigma_{\text{fit},i}) = \sum_{j=1}^3 \frac{f_j}{\sqrt{2\pi}\sigma_{ij}} \exp\left(-\frac{\delta_i^2}{2\sigma_{ij}^2}\right),$$

with $\sum_{j=1}^3 f_j = 1.$ (2)

The j th impact parameter resolution for the i th track,

σ_{ij} , was parametrised as follows:

$$\sigma_{ij}^2 = a_j^2 \sigma_{\text{fit},i}^2 + (\sigma_H^2 \sin^2 \phi_i + \sigma_V^2 \cos^2 \phi_i) + \sigma_{\text{MS}}^2 (p_{T,i}^{\text{TEC}}), \quad (3)$$

where the factors a_j are corrections to the track fit impact parameter error, $\sigma_{\text{fit},i}$. The calculation of $\sigma_{\text{fit},i}$ was corrected on a sector-by-sector basis and as a function of drift distance to ensure agreement with the impact parameter resolution measured in Bhabha and dimuon events.

The values of a_j and f_j were determined using a sample of hadron tracks with similar kinematic and topological characteristics as the inclusive lepton tracks. This sample was selected from the full hadronic event sample by applying the inclusive electron selection cuts, except for those based on the shower shape and track–shower matching quantities. Cuts were then applied to these variables to reject rather than select genuine electron candidates. In this way a sample of “anti-selected” tracks was obtained with negligible contamination from semileptonic b and c hadron decays. The impact parameters of these tracks depend on the beam spot size, the TEC resolution and, for secondary decays, on the lifetimes of b , c , and long-lived hadrons. The impact parameter resolution also depends on the track length, number of hits, and p_T^{TEC} , as well as on the isolation from other tracks, i.e. p_T^{et} and $\Delta\phi$ to the nearest TEC track. Track weights w_i were obtained which brought the normalised distributions of these five variables into agreement for the Monte Carlo anti-selected sample and the Monte Carlo prompt, cascade and charm selected lepton samples. The weights were obtained separately for electrons and muons, to allow for the isolation requirements implicit in the electron selection. Values for a_j and f_j were obtained from an unbinned maximum likelihood fit to the impact parameters of the anti-selected sample, where the log-likelihood was defined as

$$\ln \mathcal{L}(a_j, f_j) = \sum_{i \text{ tracks}} w_i \ln \left(\sum_{j=1}^3 \left(f_p + f_s \mathcal{P}_{\text{as}}(\delta_i, \tau_b) \right) \otimes \mathcal{R}(a_j, f_j; \delta_i, \phi_i, p_{T,i}^{\text{TEC}}, \sigma_{\text{fit},i}) \right), \quad (4)$$

where $f_p = 0.75$ and $f_s = 0.25$ are the fractions of tracks from the primary event vertex and from sec-

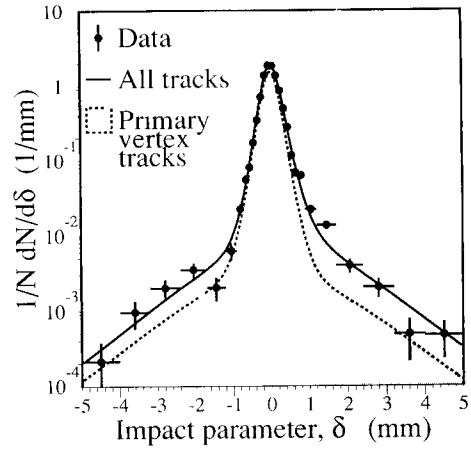


Fig. 2. The impact parameter distribution of “anti-selected” tracks used to obtain the resolution correction parameters. The points are the data and the solid line is the result of the fit described in the text. The shaded region indicates the contribution from tracks originating from the primary event vertex.

ondary decays respectively. \mathcal{P}_{as} is the underlying impact parameter distribution for secondary tracks in the anti-selected sample. The JETSET hadronic event sample was used to estimate f_p , f_s , and \mathcal{P}_{as} . Only the negative impact parameter region was used in the fit in order to reduce the sensitivity to the Monte Carlo modelling of \mathcal{P}_{as} . To correct for the difference in the Monte Carlo and measured b hadron lifetimes, the resolution and lifetime fits were performed iteratively. At each iteration a correction was applied to the underlying impact parameters of tracks from b decays which contributed to \mathcal{P}_{as} .

Fig. 2 shows the impact parameter distribution of the anti-selected tracks and the result of the fit described above. The symmetric shaded region contains the contribution of tracks from the primary event vertex. The skewing of the full distribution to positive impact parameters is due to tracks from secondary vertices. The resolution correction parameters obtained from the fit are shown in table 2.

Table 2
Resolution correction parameters

$f_1 = 78.6\%$
$f_2 = 19.7\%$
$f_3 \equiv 1 - f_1 - f_2 = 1.7\%$
$a_1 \equiv 1.0$ (fixed)
$a_2 = 2.18$
$a_3 = 12.16$

6. Background impact parameter distributions

The normalised impact parameter distribution of the anti-selected data tracks was used to describe the probability distribution $B_e(\delta)$ for the hadronic background in the electron sample. $B_e(\delta)$ was parametrised for the lifetime fit by a sum of Gaussians with exponential tails. The validity of this procedure was verified by fitting the Monte Carlo inclusive electron sample for τ_b using the actual background tracks instead of the anti-selected tracks to describe the background distribution. The lifetimes resulting from the two fits were consistent.

Since no unbiased anti-selection was possible for the muon sample, the impact parameter distribution $B_\mu(\delta)$ of the muon background was obtained by convoluting the Monte Carlo underlying distribution of the muon background tracks with the resolution function obtained from the data, on a track-by-track basis.

7. Lifetime fit results and consistency checks

The b lifetimes obtained from the electron and muon samples are $\tau_b = (1514 \pm 52)$ fs and $\tau_b = (1554 \pm 48)$ fs respectively, where the errors are statistical only. The electron and muon impact parameter distributions and fit results are shown in fig. 3. The self-consistency of the full analysis chain was verified by analysing the JETSET hadronic events as if they were the data. The results obtained were $\tau_b = (1278 \pm 28)$ fs and $\tau_b = (1318 \pm 27)$ fs for the electron and muon samples respectively, in agreement with the Monte Carlo input lifetime of $\tau_{MC} = 1310$ fs.

Fig. 4 shows the lifetimes obtained from various subsamples of the data, described below. Samples were analysed with tighter cuts applied to p_T^{JET} , p_T^{TEC} and $|\delta|$. To check for TEC biases the tracks were

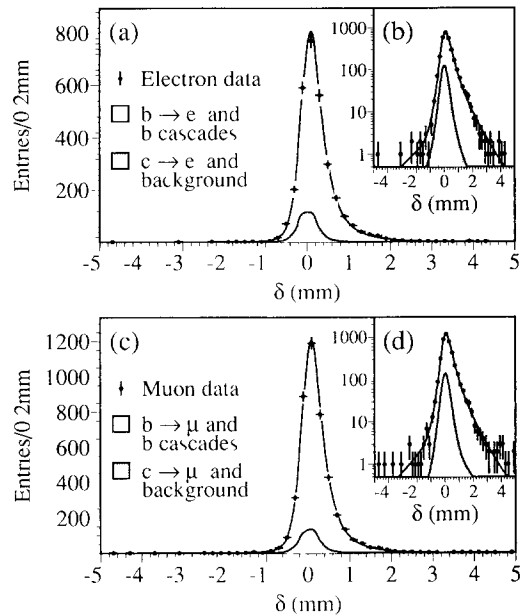


Fig. 3 Signed impact parameter distributions for electrons with (a) linear scale and (b) logarithmic scale and for muons with (c) linear scale and (d) logarithmic scale. The fits were performed using all tracks with impact parameters in the range $|\delta| < 5$ mm

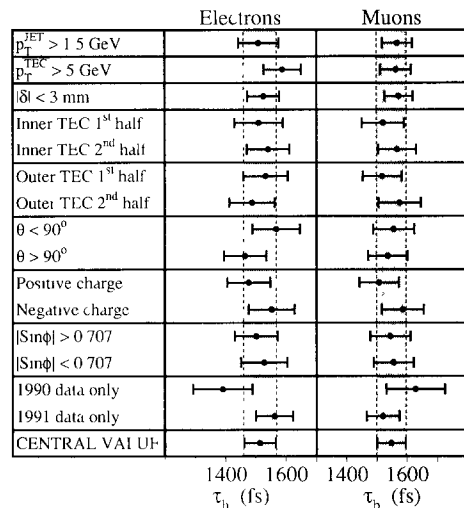


Fig. 4 Systematic cross checks of the b lifetime analysis

divided into samples depending on whether they passed closer to the anodes (1st half) or the cathodes (2nd half) of the inner and outer TEC drift volumes. Similarly, subsamples were analysed according to the

polar angle, charge, and azimuthal angle of the tracks. The data collected in 1990 and 1991 were analysed separately. No significant biases are observed. The change in the measured lifetime for the 1990 data, compared to the previously published result [4], is mainly due to the improved understanding and treatment of the impact parameter resolution function.

8. Systematic errors

The contributions to the systematic errors in the b lifetime measurements for the electron and muon samples are shown in table 3. The third column shows the combined errors allowing for correlations, where appropriate, between the two samples. Except where otherwise stated, the systematic errors of τ_b were obtained by varying the appropriate quantities within their one standard deviation errors, as described below. Errors from statistical errors on fit parameters

Table 3
Systematic errors in the τ_b measurement.

Source of systematic error	Error on τ_b (fs)		
	e	μ	e and μ
Γ_{bb}^-	± 8	± 5	± 6
Γ_{cc}^-	± 1	± 2	± 2
BR(b $\rightarrow\ell$)	± 12	± 9	± 10
BR(c $\rightarrow\ell$)	± 5	± 6	± 5
BR(b $\rightarrow c/\bar{c}\rightarrow\ell$)	± 3	± 1	± 2
BR(b $\rightarrow\tau\rightarrow\ell$)	± 1	± 1	± 1
BR(b $\rightarrow J\rightarrow\ell$)	± 1	± 2	± 1
decay model	± 9	± 7	± 8
b fragmentation function	± 14	± 8	± 10
c fragmentation function	± 2	± 2	± 2
charm hadron lifetimes	± 1	± 2	± 2
background parametrisation	± 3	± 11	± 6
background fraction	± 9	± 4	± 5
resolution parametrisation	± 16	± 16	± 16
beam spot size and position	± 4	± 3	± 4
TEC calibration systematics	± 5	± 5	± 5
underlying b $\rightarrow\ell$ fit	± 12	± 9	± 7
underlying c $\rightarrow\ell$ fit	± 1	± 2	± 1
underlying cascade fit	± 6	± 4	± 3
total	± 33	± 28	± 28

were estimated allowing for the full correlations between parameters.

8.1. Production and decay of b and c hadrons

The Standard Model values for the partial widths for $Z\rightarrow b\bar{b}$ and $Z\rightarrow c\bar{c}$ were assumed: $\Gamma_{bb}^- = (378 \pm 3)$ MeV, which is consistent with L3 measurements [16,17], and $\Gamma_{cc}^- = (296 \pm 10)$ MeV. The error in the b lifetime from the uncertainty in the b semileptonic branching ratio was estimated by varying the L3 measured value of $\text{Br}(b \rightarrow \ell\nu X) = (11.9 \pm 0.3(\text{stat.}) \pm 0.6(\text{syst.}))\%$ [17] within the statistical errors; the systematic errors affecting this measurement are considered explicitly below. An average charm semileptonic branching ratio of $\text{Br}(c \rightarrow \ell\nu X) = (10.3 \pm 1.2)\%$ was assumed. The error includes the uncertainties in the production rates of D^0 and D^\pm mesons, particularly from D^* decays, D_s^\pm mesons and charmed baryons, and the errors on the branching ratios for these different hadrons. The $b \rightarrow c/\bar{c} \rightarrow \ell$ fraction was varied by $\pm 15\%$ to allow for the uncertainties in the production and decay rates of c hadrons produced in b hadron decays. The error on the fraction of $b \rightarrow \tau \rightarrow \ell$ decays was estimated assuming: $\text{Br}(b \rightarrow \tau\nu X) = (4.1 \pm 1.0)\%$ [18], $\text{Br}(\tau \rightarrow e\nu_e\nu_\tau) = (17.58 \pm 0.27)\%$ [19] and $\text{Br}(\tau \rightarrow \mu\nu_\mu\nu_\tau) = (17.93 \pm 0.26)\%$ [19]. Similarly, for the decay $b \rightarrow J \rightarrow \ell$, the following branching ratios were varied: $\text{Br}(b \rightarrow J + X) = (1.3 \pm 0.3)\%$ [20] and $\text{Br}(J \rightarrow \ell^+\ell^-) = (5.91 \pm 0.23)\%$ [21].

To estimate the sensitivity of the analysis to the JETSET heavy quark decay model, the data were fitted using a JETSET Monte Carlo sample in which the decays of b and c hadrons were simulated with the EURODEC program [22]. The change in the b lifetime sample was used to estimate the systematic error due to the JETSET decay model. The production rates of D^{**} and K^* mesons in b and c decays were tuned within JETSET to reproduce the CLEO/ARGUS and the DELCO/MARK III lepton spectra. The statistical errors from these fits resulted in a 2 fs error on the measured lifetime. The uncertainties on the B^* and B^{**} production rates have been estimated to have a negligible influence on the sample composition [17]. The total error from the heavy quark decay model was estimated by combining the EURODEC, D^{**} , and K^* errors.

8.2. Heavy quark fragmentation

The error on the b lifetime due to the uncertainty in the b quark fragmentation was estimated by reweighting the Monte Carlo events according to Peterson functions [23] corresponding to the $\pm 1\sigma$ variations in the fraction of the beam energy imparted to the b quark, $\langle x_E \rangle_b = 0.689 \pm 0.015$ [17,20]. The string fragmentation model of JETSET was also compared with the cluster fragmentation model of the HERWIG Monte Carlo [24]; to facilitate this comparison both programs used the EURODEC decay package. The change in the lifetime was within the error assigned above. The effect of the c quark fragmentation function on the sample composition was estimated assuming a mean c quark energy fraction of $\langle x_E \rangle_c = 0.48 \pm 0.04$.

8.3. Charm hadron lifetimes

The shapes of the primordial distributions for the semileptonic decays of c hadrons depend on the lifetimes, production rates and semileptonic branching ratios [19] of the different c hadrons produced. Varying these quantities within their errors, the mean charm lifetime was estimated to be $\langle \tau_c \rangle = (690 \pm 70)$ fs.

8.4. Background distributions

The error from the electron background parametrisation was estimated by varying the fit parameters of the impact parameter distribution for the anti-selected tracks within their statistical errors. The error due to the muon background parametrisation included contributions from the statistics of the background underlying distribution and from the resolution function parametrisation, including the error in the b lifetime correction procedure. In addition, the electron and muon background fractions were each varied by $\pm 10\%$.

8.5. Resolution function

The resolution corrections, a_j and f_j , were varied within their statistical errors allowing for correlations and the uncertainty in the b lifetime correction. The size of the beam spot was varied within the measure-

ment errors and the beam centroid positions for each block of 100 events were randomly smeared in x and y with a Gaussian error of $30 \mu\text{m}$. The effects of systematic TEC calibration errors were estimated by measuring τ_b both with and without the impact parameter corrections.

8.6. Underlying distributions for prompt, cascade and charm decays

The parameters describing the underlying distributions were varied within their statistical errors. Correcting for electron bremsstrahlung reduced the lifetime obtained from the electron sample by 3 fs. The uncertainty in this correction was taken to be the full size of the correction.

9. Conclusions

In the 1990 and 1991 LEP runs 432 538 hadronic Z decays were recorded by the L3 detector at LEP. From these events, 2998 inclusive electron and 4359 inclusive muon candidates were selected with a b purity of 87%. The b hadron lifetime was obtained from fits to the lepton impact parameter distributions:

$$\tau_b = (1514 \pm 52 \pm 33) \text{ fs} \\ \text{(inclusive electron sample),}$$

$$\tau_b = (1554 \pm 48 \pm 28) \text{ fs} \\ \text{(inclusive muon sample).}$$

These results were combined, allowing for correlations in the systematic errors, to give

$$\tau_b = (1535 \pm 35 \pm 28) \text{ fs},$$

where the first error is statistical and the second is systematic. This value is an average of the lifetimes of the different b hadrons produced in Z decays weighted by their production rates and semileptonic branching ratios. It is in agreement with published data [1-3] and supersedes the previous L3 result [4].

Acknowledgement

We wish to express our gratitude to the CERN accelerator divisions for the excellent performance of the LEP machine. We acknowledge the contributions of all the engineers and technicians who have participated in the construction and maintenance of this experiment.

References

- [1] MARK II Collab., N S Lockyer et al, Phys. Rev. Lett. 51 (1983) 1316;
MAC Collab., W.W. Ash et al, Phys. Rev. Lett. 58 (1987) 640,
HRS Collab., J M Brom et al., Phys. Lett. B 195 (1987) 301,
DELCO Collab., D.E. Klem et al., Phys. Rev. D 37 (1988) 41,
MARK II Collab., R.A. Ong et al., Phys. Rev. Lett. 62 (1989) 1236.
- [2] TASSO Collab., W Braunschweig et al, Z. Phys. C 44 (1989) 1,
JADE Collab, J Hagemann et al., Z. Phys. C 48 (1990) 401
- [3] ALEPH Collab., D Decamp et al., Phys. Lett. B 257 (1991) 492;
DELPHI Collab., P. Abreu et al., Z. Phys. C 53 (1992) 567.
OPAL Collab, P D Acton et al., Phys. Lett. B 274 (1992) 513,
ALEPH Collab., D. Buskulic et al., Phys. Lett. B 295 (1992) 174,
OPAL Collab., P.D. Acton et al., CERN-PPE/93-92 (1993), submitted to Z. Phys. C
- [4] L3 Collab., B. Adeva et al., Phys. Lett. B 270 (1991) 111
- [5] W.B. Atwood and J.A. Jaros, in: B Decays, ed. S. Stone, World Scientific, Singapore (1992), p. 261
- [6] D McNally, Measurement of the Average b Hadron Lifetime with the L3 Detector at LEP, Ph D Thesis (in preparation), ETH, Zurich
- [7] L3 Collab, B. Adeva et al., Nucl. Instrum. Methods A 289 (1990) 35
- [8] F Beissel et al, Nucl. Instrum. Methods A 332 (1993) 33.
- [9] L3 Collab, B. Adeva et al., Z. Phys. C 51 (1991) 179
- [10] T. Sjostrand, Comp. Phys. Comm. 39 (1986) 347,
T Sjostrand and M Bengtsson, Comp. Phys. Comm. 43 (1987) 367,
an input value for the b lifetime of $\tau_{MC} = 1310$ fs was used
- [11] R. Brun et al, GEANT 3, CERN report DD/EE/84-1 (1984), revised (September 1987).
- [12] H Fesefeldt, RWTH Aachen report PITHA 85/02 (1985)
- [13] ARGUS Collab., H Albrecht et al., Phys. Lett. B 249 (1990) 359,
CLEO Collab, S Henderson et al, Phys. Rev. D 45 (1992) 21.
- [14] DELCO Collab., W Bacino et al., Phys. Rev. Lett. 43 (1979) 1073.
MARK III Collab., R.M. Baltrusaitis et al., Phys. Rev. Lett. 54 (1985) 1976
- [15] S. Jadach, B.F.L. Ward and Z Was, Comp. Phys. Comm. 66 (1991) 276.
- [16] L3 Collab, O. Adriani et al., Phys. Lett. B 307 (1993) 237
- [17] L3 Collab, B. Adeva et al., Phys. Lett. B 261 (1991) 177
- [18] ALEPH Collab, D. Buskulic et al., Phys. Lett. B 298 (1993) 479
- [19] Particle Data Group, Phys. Rev. D 45 (1992).
- [20] L3 Collab, O. Adriani et al., Phys. Lett. B 288 (1992) 412.
- [21] MARK III Collab., D Coffman et al, Phys. Rev. Lett. 68 (1992) 282.
- [22] A. Ali and B van Eijk, in: Z Physics at LEP 1, CERN report CERN 89-08, eds. G. Alterelli, R. Kleiss and C. Verzegnassi (CERN, Geneva, 1989), Vol. 3, p. 226.
- [23] C Peterson et al., Phys. Rev. D 27 (1983) 105.
- [24] G Marchesini and B Webber, Nucl. Phys. B 310 (1988) 461,
G. Marchesini et al., Comp. Phys. Comm. 67 (1992) 465